Finite-difference time-domain studies of low-frequency stop band in superconductor-dielectric superlattice*

Wang Shen-Yun(王身云)[a)b)†], Liu Shao-Bin(刘少斌)[a)], and Le-Wei Joshua Li[b)]

[a)] *College of Information Science and Technology, Nanjing University of Aeronautics & Astronautics, Nanjing* 210016, *China*
[b)] *Department of Electrical and Computer Engineering, National University of Singapore, Singapore* 117576, *Singapore*

(Received 23 September 2009; revised manuscript received 18 January 2010)

The transmission coefficients of electromagnetic (EM) waves due to a superconductor-dielectric superlattice are numerically calculated. Shift operator finite difference time domain (SO-FDTD) method is used in the analysis. By using the SO-FDTD method, the transmission spectrum is obtained and its characteristics are investigated for different thicknesses of superconductor layers and dielectric layers, from which a stop band starting from zero frequency can be apparently observed. The relation between this low-frequency stop band and relative temperature, and also the London penetration depth at a superconductor temperature of zero degree are discussed, separately. The low-frequency stop band properties of superconductor-dielectric superlattice thus are well disclosed.

Keywords: shift operator finite difference time domain method, superconductor, superconductor-dielectric superlattice, high-pass filter

PACC: 4110H

1. Introduction

A one-dimensional (1D) Bragg lattice is a spatially periodical structure. Much attention was paid to the periodic multilayered structure, where different materials such as dielectrics, semiconductors, metals and plasma media were commonly utilized.[1−6] There are usually many forbidden band gaps due to this 1D stratified medium of finite period but infinite number of layers. The band gap of a dielectric–dielectric superlattice can be broadened significantly by increasing the contrast of neighbouring dielectric permittivities. A low-frequency band gap (below the first band gap) can be easily found from a metal–dielectric superlattice, and its gap width primarily depends on the plasma frequency of metals.[5,6]

In addition, the Bragg lattices of superconductor and dielectric also attracted much attention recently.[7−10] For instance, a 1D superconductor-dielectric superlattice was considered in Ref. [7]. By making use of the transfer matrix method and the Bloch theorem, a low-frequency band gap was apparently observed from the analysis in the case of plane wave incidences in both transversal magnetic (TM) and transversal electric (TE) modes.

Due to the existence of the low-frequency band gap, this 1D superconductor-dielectric superlattice can be practically applied to a high-pass filter. The advantage of this superconductor structure is its low loss which is much less than that of a metallic superlattice, because the imaginary part in the dielectric constant of superconductor is much less than that of metalic material.[8]

In the present paper, we apply the shift operator finite difference time domain (SO-FDTD) method to the superconductor structure. For validation purpose, the results from the method are compared with the analytical solutions by calculating the transmission and reflection coefficients of a superconductor slab, and then this new FDTD formulation is used to calculate the low-frequency stop band of superconductor-dielectric superlattice. We also discuss the dependence of the low-frequency stop band on superconductor parameters and superlattice structure.

2. SO-FDTD method for superconductor

For a dispersive medium, Maxwell's curl equations and the constitutive relation equation are given

*Project supported partly by the Open Research Program in State Key Laboratory of Millimeter Waves of China (Grant No. K200802), and partly by the National Natural Science Foundation of China (Grant No. 60971122).
†Corresponding author. E-mail: wangsy@126.com
© 2010 Chinese Physical Society and IOP Publishing Ltd

as follows:

$$\frac{\partial \boldsymbol{D}}{\partial t} = \boldsymbol{\nabla} \times \boldsymbol{H}, \tag{1}$$

$$\frac{\partial \boldsymbol{H}}{\partial t} = -\frac{1}{\mu_0}\boldsymbol{\nabla} \times \boldsymbol{E}, \tag{2}$$

$$\boldsymbol{D}(\omega) = \varepsilon_0 \varepsilon_{\rm r}(\omega)\boldsymbol{E}(\omega). \tag{3}$$

The two-fluid model[8] is used to describe the electrodynamics of superconductor at a nonzero temperature. With some approximations, the complex conductivity of the superconductor can be written as

$$\sigma = -{\rm i}\frac{1}{\omega\mu_0\lambda_{\rm L}^2}. \tag{4}$$

The conditions for a lossless superconductor are described in Ref. [8] in detail. Then the dielectric response function is

$$\varepsilon_{\rm r}(\omega) = 1 - \frac{1}{\omega^2\mu_0\varepsilon_0\lambda_{\rm L}^2}, \tag{5}$$

where the temperature-dependent penetration depth is given by

$$\lambda_{\rm L} = \lambda_{\rm L}(T) = \lambda_{\rm L}(0)\left\{1 - \left(\frac{T}{T_{\rm c}}\right)^4\right\}^{-1/2}, \tag{6}$$

where T and $T_{\rm c}$ are the temperatures of sample and phase transformation of superconductor, respectively; $\lambda_{\rm L}(T)$ and $\lambda_{\rm L}(0)$ are the London penetration depths at temperature T and zero temperature, respectively; $\omega_{\rm p}$ is the plasma frequency and usually defined as

$$\omega_{\rm p}^2 = \frac{c^2}{\lambda_{\rm L}(0)^2}\left\{1 - \left(\frac{T}{T_{\rm c}}\right)^4\right\}. \tag{7}$$

Thus, the dielectric constant of superconductor is similar in form to that of a free-electron metal. Then we rewrite the response function in Eq. (5) as a rational fractional function

$$\varepsilon_{\rm r}(\omega) = \frac{\sum_{n=0}^{N} p_n({\rm i}\omega)^n}{\sum_{n=0}^{N} q_n({\rm i}\omega)^n}. \tag{8}$$

Comparing the response functions in Eqs. (8) and (5), we see that summation number N in Eq. (8) is taken to be 2. Correspondingly, the coefficients in Eq. (8) become $p_0 = \omega_{\rm p}^2$, $p_1 = 0$, $p_2 = 1$, $q_0 = 0$, $q_1 = 0$, and $q_2 = 1$. For a simple one-dimensional case, taking the central difference approximation for both temporal and spatial derivatives at $(n+0.5)\Delta t$ and $(k+0.5)\Delta z$, equations (1) and (2) turn into the following forms:

$$\begin{aligned} & H_y^{n+0.5}(k+0.5) \\ = \; & H_y^{n-0.5}(k+0.5) \\ & - \frac{\Delta t}{\mu_0 \Delta z}\left[E_x^n(k+1) - E_x^n(k)\right], \end{aligned} \tag{9}$$

$$\begin{aligned} & D_x^{n+1}(k) \\ = \; & D_x^n(k) - \frac{\Delta t}{\Delta z}[H_y^{n+0.5}(k+0.5) \\ & - H_y^{n+0.5}(k-0.5)]. \end{aligned} \tag{10}$$

The SO-FDTD method was first proposed in Ref. [11] where the relationship between E_x and D_x was obtained and the formula of E_x is given now by

$$\begin{aligned} E_x^{n+1}(k) = \; & \frac{1}{b_0}\Bigg\{a_0\left(\frac{D_x^{n+1}(k)}{\varepsilon_0}\right) \\ & + a_1\left(\frac{D_x^n(k)}{\varepsilon_0}\right) + a_2\left(\frac{D_x^{n-1}(k)}{\varepsilon_0}\right) \\ & - b_1 E_x^n(k) - b_2 E_x^{n-1}(k)\Bigg\}, \end{aligned} \tag{11}$$

where the coefficients for the superconductor structure are given below

$$a_0 = q_0 + q_1\frac{2}{\Delta t} + q_2\left(\frac{2}{\Delta t}\right)^2 = \left(\frac{2}{\Delta t}\right)^2,$$

$$a_1 = 2q_0 - 2q_2\left(\frac{2}{\Delta t}\right)^2 = -2\left(\frac{2}{\Delta t}\right)^2,$$

$$a_2 = q_0 - q_1\frac{2}{\Delta t} + q_2\left(\frac{2}{\Delta t}\right)^2 = \left(\frac{2}{\Delta t}\right)^2,$$

$$b_0 = p_0 + p_1\frac{2}{\Delta t} + p_2\left(\frac{2}{\Delta t}\right)^2 = \omega_{\rm p}^2 + \left(\frac{2}{\Delta t}\right)^2,$$

$$b_1 = 2p_0 - 2p_2\left(\frac{2}{\Delta t}\right)^2 = \omega_{\rm p}^2 - 2\left(\frac{2}{\Delta t}\right)^2,$$

$$b_2 = p_0 - p_1\frac{2}{\Delta t} + p_2\left(\frac{2}{\Delta t}\right)^2 = \omega_{\rm p}^2 + \left(\frac{2}{\Delta t}\right)^2.$$

Using the difference equations in Eqs. (9), (10) and (11), the E_x expression can be obtained and calculated by the iterative process.

3. Results and discussion

To check the accuracy of this numerical method for superconductor structure considered in Section 2, we first calculate the transmission coefficient and the reflection coefficient of a superconductor slab with a

thickness of 1000 nm as shown in Fig. 1. The superconductor is taken as niobium (Nb), and its phase transformation temperature is $T_{\rm C} = 9.2$ K (relative temperature $T/T_{\rm C} = 0.46$ is used in calculations) and its London penetration depth at zero temperature is $\lambda_{\rm L}(0) = 83.4$ nm. The normal incident wave on the superconductor slab, assumed in the simulation, is a Gaussian derivative pulsed plane wave. The computational domain considered has $1026\Delta z$ in the z-direction, where Δz is the mesh width taken as $\Delta z = 1$ nm. The time step taken is $\Delta t = 2.5\times10^{-16}$ s. The slab occupies the middle 1000 meshes, and the terminative five meshes are perfectly matched layer (PML)[12] medium and the other region is free space. The transmission coefficient and the reflection coefficient are calculated by using the fast Fourier transform (FFT) method and the simulation is allowed to run for 400000 time steps.

Figure 2 illustrates the magnitudes of the transmission coefficient and the reflection coefficient computed by applying the SO-FDTD method to the superconductor slab. It is seen that the results from an exact analytical solution and the SO-FDTD method are in good agreement with each other.

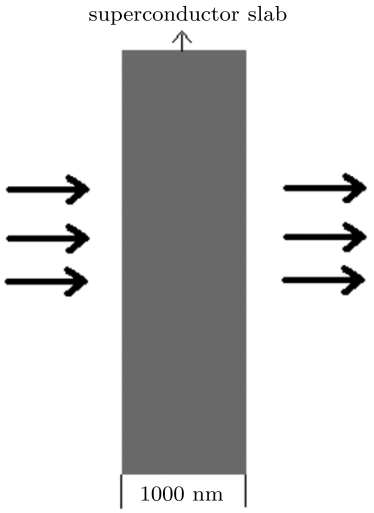


Fig. 1. Superconductor slab.

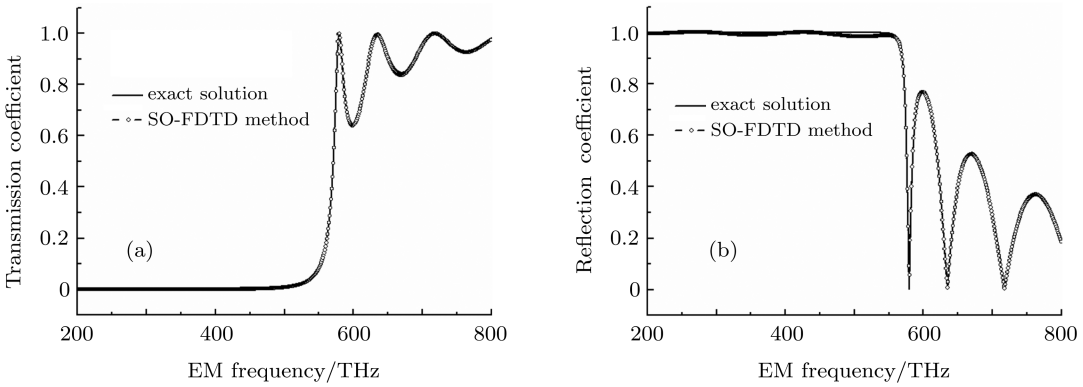


Fig. 2. Curves for transmission coefficient (a) and reflection coefficient (b) versus frequency for the superconductor with a thickness of 1000 nm at $T/T_{\rm C} = 0.46$ and $\lambda_{\rm L}(0) = 83.4$ nm, obtained by the analytical approach and the SO-FDTD method.

In what follows, we design a superconductor-dielectric twin-layer structure in the z-direction with 60 unit cells as shown in Fig. 3. The dielectric layers are considered to be lossless and simple matter, and its relative permittivity is taken as 10. The superconductor layer is assumed to be niobium with the same parameters as those, but for thickness, of the slab given above. The FDTD parameters applied to superconductor layers are also the same as those of the above slab, and the conventional FDTD formula is also applied to the dielectric layer. The computational domain varies with the total size of this superlattice, and it depends on the thicknesses of superconductor layer and dielectric layer, and on the number of unit cells.

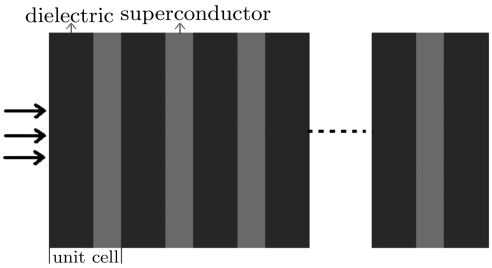


Fig. 3. Superconductor-dielectric superlattice.

Figure 4 depicts the calculated transmission coef-

ficients for different thicknesses of superconductor layers $D_S = 12$ nm, 16 nm, and 20 nm, respectively, while the fixed thickness of dielectric layer is assumed to be $D_d = 60$ nm. The cut-off frequencies are denoted by $f_{c1} = 74.8$ THz, $f_{c2} = 86.4$ THz, and $f_{c3} = 96.8$ THz, corresponding to different thicknesses given above. It can be seen that at the frequencies below the cut-off frequency, the EM wave is forbidden to propagate, which means that this periodic superconductor-dielectric superlattice behaves as a high-pass filter and the cut-off frequency is located in terahertz zone. It can also be directly noticed that the width of this low-frequency stop band becomes large when the thickness of the superconductor layer increases as shown in Fig. 4. Taking a constant thickness of the superconductor layer as $D_S = 10$ nm, we calculate the transmittance spectra for different thicknesses of dielectric layers as shown in Fig. 5. By increasing the thickness of the dielectric layer, the cut-off frequency shifts towards the lower frequency side, that is, the low-frequency stop band becomes narrower, which is contrary to the case of increasing the thickness of superconductor layer. It is important to point out that the contribution of the superconductor layer to optical thickness of a unit cell is negative at a low frequency, but the contribution of the dielectric layer to optical thickness of a unit cell is positive. This is why the cut-off frequency of the low-frequency stop band shifts reversely by increasing the thicknesses of the superconductor layer and dielectric layer.

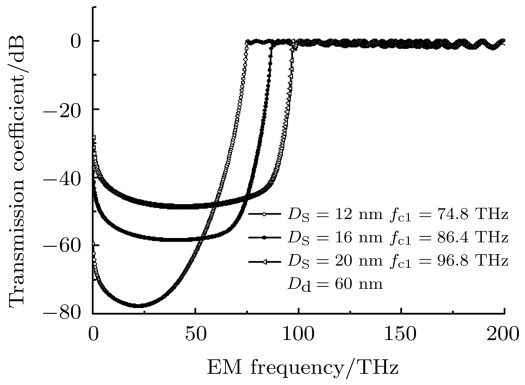


Fig. 4. Transmission coefficients at different thicknesses of superconductor layers $D_S = 12$ nm, 16 nm and 20 nm, respectively, with the thickness of dielectric layer assumed to be $D_d = 60$ nm.

To characterize the dependence of low-frequency band gap on the parameters of superconductor, we assume the thicknesses of dielectric layer and superconductor layer to be $D_d = 60$ nm and $D_S = 20$ nm, respectively. The dependence of the of the low-frequency stop band of this periodic structure on relative temperature T/T_C and London penetration depth at zero temperature $\lambda_L(0)$ are shown in Figs. 6 and 7, respectively.

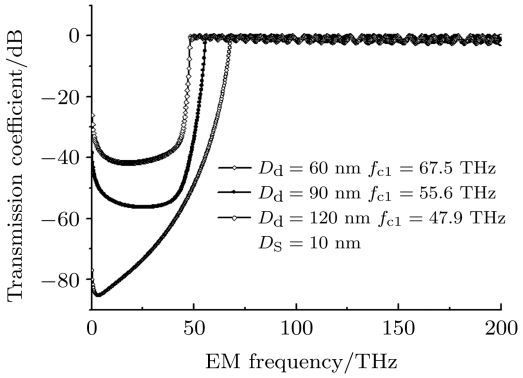


Fig. 5. Transmission coefficients at different thicknesses of dielectric layers $D_d = 60$ nm, 90 nm and 120 nm, respectively, with the thickness of superconductor layer assumed to be $D_S = 10$ nm.

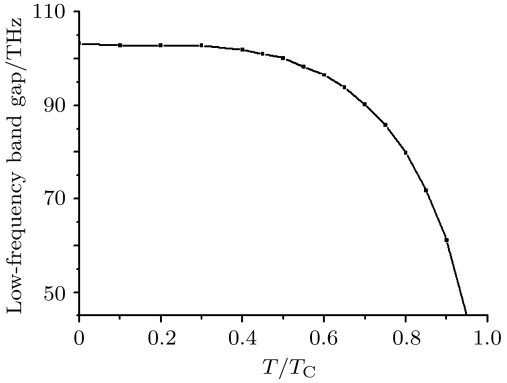


Fig. 6. Dependence of width of stop band on relative temperature T/T_C.

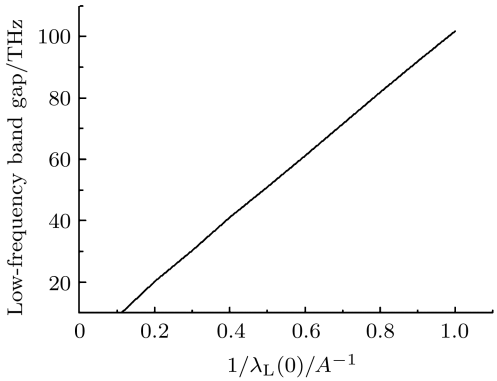


Fig. 7. Dependence of width of low-frequency band gap on reciprocal of $\lambda_L(0)$.

In the calculation of Fig. 6, the London penetration depth at zero temperature is set as $\lambda_L(0) = A = 80$ nm, where A is the period of the superlattice. It is noticed that the stop band becomes narrower with the increase of relative temperature and the maximal

cut-off frequency of the stop band is 103.2 THz at $T/T_{\rm C} = 0$. Clearly, this property can serve as the basis for a temperature-controlled high pass filter. The relationship between the width of low-frequency stop band and reciprocal of $\lambda_{\rm L}(0)$ is nearly linear as shown in Fig. 7, where the abscissa is scaled by $1/A$ and the relative temperature is taken as $T/T_{\rm C} = 0.4$ in this simulation. In fact, there exists a low-frequency band gap for EM wave in bulk superconductor. It means that when the EM frequency is lower than the plasma frequency of superconductor, the relative permittivity of superconductor becomes negative and the EM wave cannot propagate through a bulk superconductor. But the cut-off frequency of the low-frequency stop band is considerably lower than the plasma frequency of superconductor, so a conclusion can be drawn that the low-frequency stop band results from the hybrid effects of both plasma frequency of superconductor material and the periodicity of this superlattice.

4. Conclusions

Using the SO-FDTD method, we calculated the transmission coefficients of superconductor-dielectric superlattice for different thicknesses of superconductor layer and dielectric layer. It is found that there exists a low-frequency stop band ranging from zero frequency to a cut-off frequency in a terahertz zone. We also discussed the relationship between low-frequency stop band and relative temperature, and London penetration depth at zero temperature of superconductor. Two conclusions can be drawn as follows. First, the cut-off frequency of the low-frequency stop band shifts reversely by increasing the thickness of superconductor layer and the thickness of dielectric layer, which is due to their contributions contrary to optical thickness of a unit cell. Second, we can broaden the low-frequency stop band by reducing the relative temperature $T/T_{\rm c}$ or London penetration depth at zero temperature $\lambda_{\rm L}(0)$ of superconductor. The conclusions might be useful for actually designing bandpass filters and other photonic crystal applications.

References

[1] Liu N H 1997 *Phys. Rev.* B **55** 4097

[2] Xu X S, Xiong Z G, Jin A Z, Chen H D and Zhang D Z 2007 *Acta Phys. Sin.* **56** 916 (in Chinese)

[3] Liu S B, Zhu C X and Yuan N C 2005 *Acta Phys. Sin.* **54** 2804 (in Chinese)

[4] Wang S Y and Liu S B 2009 *Acta Phys. Sin.* **58** 7062 (in Chinese)

[5] Dong J W, Hu X H and Wang H Z 2007 *Chin. Phys.* **16** 1057

[6] McGurn A R and Maradudin A A 1993 *Phys. Rev.* B **48** 17576

[7] Raymond Ooi C H and Au Yeung T C 1999 *Phys. Lett.* A **259** 413

[8] Raymond Ooi C H, Au Yeung T C, Kam C H and Lim T K 2000 *Phys. Rev.* B **61** 5920

[9] Chen Y B, Zhang C, Zhu Y Y, Zhu S N and Ming N B 2002 *Mater. Lett.* **55** 12

[10] Wu C J, Chen M S and Yang T J 2005 *Physica* C **432** 133

[11] Ge D B, Wu Y L and Zhu X Q 2003 *Chin. J. Radio Sci.* **18** 359 (in Chinese)

[12] Berenger J P 1994 *J. Comput. Phys.* **114** 185